연구논문

Journal of Drive and Control, Vol.17 No.2 pp.28-37 Jun. 2020
ISSN 2671-7972(print) ISSN 2671-7980(online)
http://dx.doi.org/10.7839/ksfc.2020.17.2.028

Analysis on Torque, Flowrate, and Volumetric Displacement of Gerotor Pump/Motor

Hongsik Yun[1], Young-Bog Ham[2] and Sungdong Kim[1*]

Received: 02 Apr. 2020, Revised: 14 May 2020, Accepted: 18 May 2020

Key Words : Torque Equilibrium, Energy Conservation, Volumetric Displacement, Flowrate, Rotation Speed, Gerotor Pump/Motor

Abstract: It is difficult to analytically derive the relationship among volumetric displacement, flowrate, torque, and rotation speed regarding an instantaneous position of gerotor hydraulic pumps/motors. This can be explained by the geometric shape of the rotors, which is highly complicated. Herein, an analytical method for the instantaneous torque, rotation speed, flowrate, and volumetric displacement of a pump/motor is proposed. The method is based on two physical concepts: energy conservation and torque equilibrium. The instantaneous torque of a pump/motor shaft is determined for the posture of rotors from the torque equilibrium. If the torque equilibrium is combined with the energy conservation between the hydraulic energy of the pump/motor and the mechanical input/output energy, the formula for determining the instantaneous volumetric displacement and flowrate is derived. The numerical values of the instantaneous volumetric displacement, torque, rotation speed, and flowrate are calculated via the MATLAB software programs, and they are illustrated for the case in which inner and outer rotors rotate with respect to fixed axes. The degrees of torque fluctuation, speed fluctuation, and flowrate fluctuation can be observed from their instantaneous values. The proposed formula may provide a better understanding of the design or analysis process of gerotor pumps/motors.

Nomenclature

e : eccentricity between centers of inner and outer rotors
F_k : force induced by pressure distribution
m : number of outer rotor's lobes
p : coordinates of pitch point
$Q(t)$: instantaneous flow rate
r_c : radius of outer rotor's circular part
r_t : distance from the center of outer rotor to the center of circular part
R_k : contact force
T_L : load torque on a pump/motor shaft
$V_{2\pi}$: volumetric displacement per revolution

Subscripts

1 : inner rotor
2 : outer rotor

1. Introduction

Gerotor gears have been used for small-sized pumps and high-torque hydraulic motors. They produce an internal contact movement and rotate at a speed that is inversely proportional to the number of lobes (or gears) of the outer rotors, thereby maintaining the centers and

* Corresponding author: sdkim@kumoh.ac.kr
1 Department of Mechanical System Engineering, Kumoh National Institute of Technology, Gumi 39177, Korea
2 Energy Systems Research Division, KIMM, Deajeon 34103, Korea

pitch point of the inner and outer rotors fixed in space. Circular arc curves are generally used as lobe profiles of outer rotors for design and processing convenience. The shapes of the inner rotors are generated by the gear profiles of the outer rotors and exhibit a trochoid curve[1-4].

Generally, gerotor hydraulic pumps/motors exhibit highly complicated geometric shapes, which complicate the calculation of their volumetric displacements using geometric methods. Previous studies[5-7] have proposed methods for calculating the volumetric displacement by directly calculating the chamber volume between the contact points of the inner and outer rotors. The procedures and formulas of this method are highly complicated; therefore, the method is difficult to reflect in design. For example, the flowrate of pumps/motors and the torque and rotation speed of pump/motor shafts are difficult to calculate.

Many studies[8-13] have introduced formulas for calculating volumetric displacement using the contact point lengths of inner and outer rotors (hereinafter, vane length). The vane length method is based on kinematic analysis of the inner and outer rotors' motion, and thus, it is hard to understand how the pressure and contact forces between the rotors affect the instantaneous torque of the pump/motor shaft. The vane length method is also hard to give relations among torque, flowrate and volumetric displacement of the gerotor pump/motors.

This study considered a method for calculating the instantaneous volume change rate, rotation speed, and torque of pumps/motors based on two concepts: the torque equilibrium of the rotors and energy conservation between the hydraulic energy of pumps/motors and mechanical energy of driving shafts. The torque of the pump/motor is derived from the torque equilibrium, which may provide direct insight into the torque and show how the pressure and contact forces affect the instantaneous torque fluctuation. The formula equations about the instantaneous flowrate, rotor speed and volumetric displacement of the pump/motor are also derived from combining the torque equilibrium with the energy conservation equation. The contact points between the inner and outer rotors should be used in the calculation process of volumetric displacement. The calculation to obtain the contact points is also introduced. This study was conducted for the case of rotating inner and outer rotors, as shown in Fig. 1. The centers of the rotors, O_1 and O_2, and the pitch point, p, were assigned as spatially constant points. The numerical values of the instantaneous volumetric displacement, torque, rotation speed, and flowrate were calculated via MATLAB software programs, and they are illustrated herein for the case in which the inner and outer rotors rotate with respect to the fixed axes. The degrees of torque, speed, and flowrate fluctuations were observed from the instantaneous values of torque, speed, and flowrate, respectively.

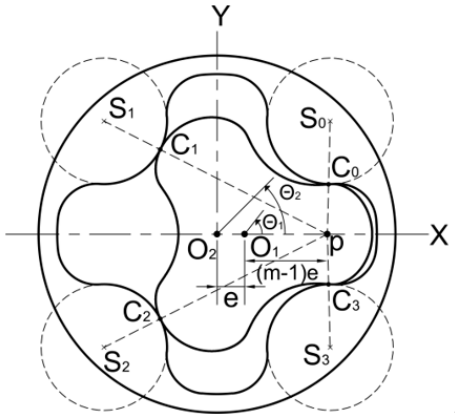

Fig. 1 Rotation of inner and outer rotors

2. Torque, volumetric displacement, and flowrate

2.1 Energy conservation

The energy conservation principle was applied between the hydraulic energy and the mechanical torque energy in the hydraulic pump/motor, as shown in Fig. 2. For the convenience of interpretation, we assumed that the efficiency was ideally 100%, the pressure of the high-pressure section was P, and that of the low-pressure section was 0.

Based on these assumptions, we derived the energy conservation equation with respect to the rotation of the pump/motor shaft by $\Delta\theta_1$, as follows:

$$T_L \cdot \Delta\theta_1 = P \cdot \Delta V \tag{1}$$

where T_L is the load torque on the pump/motor

shaft, ΔV the volumetric displacement or supply volume of fluid with respect to the rotation by $\Delta\theta_1$, and P the supply pressure.

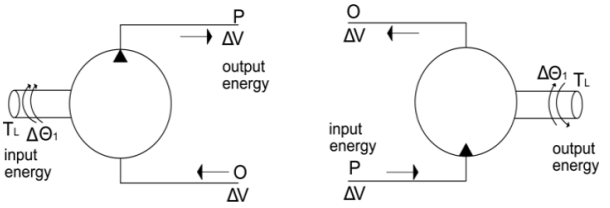

a) pump b) motor

Fig. 2 Hydraulic energy and shaft torque energy of pump/motors

2.2 Torque equilibrium

The load torque, T_L, can be obtained as a function of the pressure, P, from the torque equilibrium equation with respect to the free-body diagram of the inner and outer rotors, as shown in Figs. 3 and 4. Although a slight difference existed according to whether the driving axis of the pump/motor is connected to the inner rotor or to the outer rotor, we assumed that the driving axis was connected to the inner rotor because of its similarity to the development process of interpretation.

In Fig. 3 and 4, R_k is the force on the contact point, C_k, of the inner and outer rotors, and F_k is the hydraulic force by the pressure, P. The contact and hydraulic forces, which act on the inner and outer rotors, respectively, establish the relationship between the force and reaction force, creating a pair; hence, although their action points and sizes are identical, they act in opposite directions from the inner and outer rotors. The effect of hydraulic force on the cross section is dependent on the projected area of the cross section and is independent of the shape of the cross section; it can be expressed as follows:

$$F_k = P_k b L_{C_iC_j} \text{ for } k = 0, 1, 2, \cdots, m-1 \tag{2}$$

$$L_{C_iC_j} = \sqrt{(X_{C_j} - X_{C_i})^2 + (Y_{C_j} - Y_{C_i})^2} \tag{3}$$

where $L_{C_iC_j}$ is the distance between the adjacent contact points C_i and C_j, b is the thickness of the inner and outer rotors, m is number of the outer rotor's lobes, and subscript k means the kth chamber.

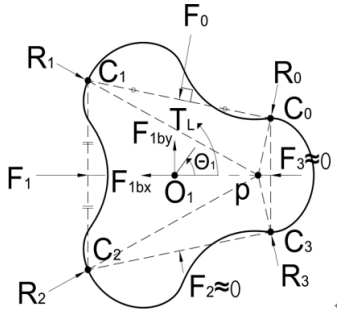

Fig. 3 Free-body diagram of the inner rotor

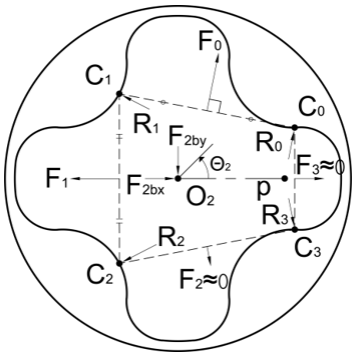

Fig. 4 Free-body diagram of the outer rotor

As shown in Fig. 5, the effect of torque by the hydraulic force between C_i and C_j can be expressed with respect to the centers, O_1 and O_2, respectively, as follows:

$$T_{FO_1k} = Pb\left[\begin{array}{l}\left(Y_{C_j} - Y_{C_i}\right)\left(\dfrac{Y_{C_j} + Y_{C_i}}{2} - Y_{O_1}\right) \\ +\left(X_{C_j} - X_{C_i}\right)\left(\dfrac{X_{C_j} + X_{C_i}}{2} - X_{O_1}\right)\end{array}\right] \tag{4}$$

$$T_{FO_2k} = -Pb\left[\begin{array}{l}\left(Y_{C_j} - Y_{C_i}\right)\left(\dfrac{Y_{C_j} + Y_{C_i}}{2} - Y_{O_2}\right) \\ +\left(X_{C_j} - X_{C_i}\right)\left(\dfrac{X_{C_j} + X_{C_i}}{2} - X_{O_2}\right)\end{array}\right] \tag{5}$$

In equation (5), the first " - " represents the opposite direction from that of the torque acting on the inner rotor. $Pb\left(Y_{C_j} - Y_{C_i}\right)$ and $Pb\left(X_{C_j} - X_{C_i}\right)$ represent the hydraulic force components in the x- and y- directions, respectively; $\dfrac{Y_{C_j} + Y_{C_i}}{2}$ and $\dfrac{X_{C_j} + X_{C_i}}{2}$ are the

coordinates of the centers of the hydraulic force; $\left(\frac{Y_{C_j}+Y_{C_i}}{2}-Y_O\right)$ and $\left(\frac{X_{C_j}+X_{C_i}}{2}-X_O\right)$ are the lengths of the moment arm with respect to the rotation centers of the inner and outer rotors, respectively.

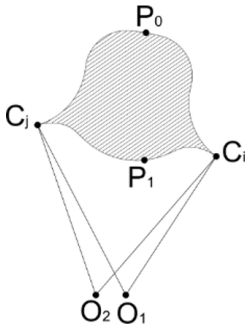

Fig. 5 Volume of a chamber between two contact points and C_i and C_j

In the free-body diagram shown in Fig. 3, the horizontal and vertical components of the contact force, R_k, and the hydraulic force, F_k, achieve equilibrium with the support force of the bearing. However, in this case, the bearing force can be disregarded because it is not a parameter of interest. The moment equilibrium equation with respect to the center of the inner rotor, O_1, is expressed in the form of equilibrium between the load torque T_L and the sum of the torque effect of the hydraulic force F_k, $\sum T_{FO_1k}$, and that of the contact force R_k of the lobes of the outer rotor, $\sum T_{RO_1k}$, is expressed as follows:

$$T_L=\sum_{k=0}^{h}T_{FO_1k}+\sum_{k=0}^{h}T_{RO_1k} \tag{6}$$

where h is the number of chambers of the high-pressure section on which the pressure, P, of the high-pressure section acts.

Because the load torque, T_L, does not act on the torque equilibrium of the outer rotor, as shown in the free-body diagram in Fig. 4, the torque effect of the hydraulic force enters equilibrium with that of the contact force; that is, the reaction torque transferred through the contact points from the inner rotor, $\sum T_{RO_2k}$, has the same magnitude as that of the hydraulic force, $\sum T_{FO_2k}$.

$$\sum_{k=0}^{h}T_{RO_2k}=\sum_{k=0}^{h}T_{FO_2k} \tag{7}$$

The torque generated from the outer rotor, $\sum T_{RO_2k}$, is transferred to the inner rotor in the proportion of the pitch radius of the inner rotor, r_1, to the pitch radius of the outer rotor, r_2. Additionally, the proportion of r_1 to r_2 is proportional to the number of lobes of the inner and outer rotors.

$$\sum_{k=0}^{h}T_{RO_1}=\frac{r_1}{r_2}\sum_{k=0}^{h}T_{RO_2}=\frac{m-1}{m}\sum_{k=0}^{h}T_{RO_2} \tag{8}$$

Rearranging equations (7) and (8) and substituting into equation (6) yields

$$T_L=\sum_{k=0}^{h}T_{FO_1k}+\frac{m-1}{m}\sum_{k=0}^{h}T_{FO_2k} \tag{9}$$

Substituting equations (4) and (5) into equation (9) yields

$$\begin{aligned}T_L=&\sum_{k=0}^{h}Pb\left[\left(Y_{C_j}-Y_{C_i}\right)\left(\frac{Y_{C_j}+Y_{C_i}}{2}-Y_{O_1}\right)\right.\\&\left.+\left(X_{C_j}-X_{C_i}\right)\left(\frac{X_{C_j}+X_{C_i}}{2}-X_{O_1}\right)\right]\\&-\frac{m-1}{m}\sum_{k=0}^{h}Pb\left[\left(Y_{C_j}-Y_{C_i}\right)\left(\frac{Y_{C_j}+Y_{C_i}}{2}-Y_{O_2}\right)\right.\\&\left.+\left(X_{C_j}-X_{C_i}\right)\left(\frac{X_{C_j}+X_{C_i}}{2}-X_{O_2}\right)\right]\end{aligned} \tag{10}$$

Many contact points equal to the number of lobes of the outer rotor emerge between the inner and outer rotors, as shown in Fig. 3 and 4. Assuming that the chambers emerging from the contact points from C_0 to C_h are high-pressure chambers, the torque effect of all high-pressure chambers, $\sum T_k$, can be expressed using only the initial and final contact points of the high-pressure section, C_0 and C_h, respectively. This is because the C_i coordinate of a high-pressure chamber corresponds to C_j of the next high-pressure chamber, and they offset each other. Equation (10) simplifies this as follows:

$$T_L = Pb\begin{bmatrix}\left(Y_{C_h\max}-Y_{C_0\min}\right)\left(\dfrac{Y_{C_h\max}+Y_{C_0\min}}{2}-Y_{O_1}\right)\\ +\left(X_{C_h\max}-X_{C_0\min}\right)\left(\dfrac{X_{C_h\max}+X_{C_0\min}}{2}-X_{O_1}\right)\end{bmatrix}$$
$$-\frac{m-1}{m}Pb\begin{bmatrix}\left(Y_{C_h\max}-Y_{C_0\min}\right)\left(\dfrac{Y_{C_h\max}+Y_{C_0\min}}{2}-Y_{O_2}\right)\\ +\left(X_{C_h\max}-X_{C_0\min}\right)\left(\dfrac{X_{C_h\max}+X_{C_0\min}}{2}-X_{O_2}\right)\end{bmatrix} \quad (11)$$

where $(X_{C_h\max}, Y_{C_h\max})$ is the farthest contact point from the pitch point, C_h; $(X_{C_0\min}, Y_{C_0\min})$ is the nearest contact point, C_0; h is the number of high-pressure chambers; h is equal to $m/2$ if the number of lobes of the outer rotor, m, is an even number. By contrast, if m is an odd number, it can be expressed as a function of the rotation of the inner rotor, θ_1, as follows:

$$h=\begin{cases}\dfrac{m-1}{2} & \text{for } \dfrac{2k\pi}{m-1}\le\theta_1\le\dfrac{(2k+1)\pi}{m-1}\\ \dfrac{m+1}{2} & \text{for } \dfrac{(2k+1)\pi}{m-1}\le\theta_1\le\dfrac{(2k+2)\pi}{m-1}\end{cases}$$
$$\text{for } k=0,1,2,\cdots,m-1 \quad (12)$$

2.3 Volumetric displacement and flowrate of pump/motors

By substituting equation (11) into equation (1), the volume change rate of fluid with respect to the rotation by $\Delta\theta_1$, $\Delta V/\Delta\theta_1$, can be obtained as follows:

$$\frac{\Delta V}{\Delta\theta_1}=b\begin{bmatrix}\left(Y_{C_h\max}-Y_{C_0\min}\right)\left(\dfrac{Y_{C_h\max}+Y_{C_0\min}}{2}-Y_{O_1}\right)\\ +\left(X_{C_h\max}-X_{C_0\min}\right)\left(\dfrac{X_{C_h\max}+X_{C_0\min}}{2}-X_{O_1}\right)\end{bmatrix}$$
$$-\frac{m-1}{m}b\begin{bmatrix}\left(Y_{C_h\max}-Y_{C_0\min}\right)\left(\dfrac{Y_{C_h\max}+Y_{C_0\min}}{2}-Y_{O_2}\right)\\ +\left(X_{C_h\max}-X_{C_0\min}\right)\left(\dfrac{X_{C_h\max}+X_{C_0\min}}{2}-X_{O_2}\right)\end{bmatrix} \quad (13)$$

The volume change rate, $\Delta V/\Delta\theta_1$, represents the instantaneous volume change rate with respect to the instantaneous rotation angle of the rotor.

The average value of the volume change rates of all high-pressure chambers, $(\Delta V/\Delta\theta_1)_{avg}$, is obtained by integrating equation (13) for the range of angles in equation (12) and dividing the integrated values by the corresponding angles.

$$\frac{\Delta V}{\Delta\theta_{1avg}}=b\int_0^{2\pi/(m-1)}\frac{\Delta V}{\Delta\theta_1}d\theta_1/[2\pi/(m-1)]=\frac{(m-1)b}{2\pi}$$
$$\cdot\int_0^{\frac{2\pi}{m-1}}\begin{bmatrix}\left(Y_{C_h\max}-Y_{C_0\min}\right)\left(\dfrac{Y_{C_h\max}+Y_{C_0\min}}{2}-Y_{O_1}\right)\\ +\left(X_{C_h\max}-X_{C_0\min}\right)\left(\dfrac{X_{C_h\max}+X_{C_0\min}}{2}-X_{O_1}\right)\end{bmatrix}$$
$$-\frac{m-1}{m}\begin{bmatrix}\left(Y_{C_h\max}-Y_{C_0\min}\right)\left(\dfrac{Y_{C_h\max}+Y_{C_0\min}}{2}-Y_{O_2}\right)\\ +\left(X_{C_h\max}-X_{C_0\min}\right)\left(\dfrac{X_{C_h\max}+X_{C_0\min}}{2}-X_{O_2}\right)\end{bmatrix}d\theta_1 \quad (14)$$

In addition, the volumetric displacement per rotation, $V_{2\pi}$, is obtained by multiplying Formula (14) by one rotation, 2π rad.

$$V_{2\pi}=\frac{\Delta V}{\Delta\theta_{1avg}}\cdot 2\pi=(m-1)b$$
$$\cdot\int_0^{\frac{2\pi}{m-1}}\begin{bmatrix}\left(Y_{C_h\max}-Y_{C_0\min}\right)\left(\dfrac{Y_{C_h\max}+Y_{C_0\min}}{2}-Y_{O_1}\right)\\ +\left(X_{C_h\max}-X_{C_0\min}\right)\left(\dfrac{X_{C_h\max}+X_{C_0\min}}{2}-X_{O_1}\right)\end{bmatrix}$$
$$-\frac{m-1}{m}\begin{bmatrix}\left(Y_{C_h\max}-Y_{C_0\min}\right)\left(\dfrac{Y_{C_h\max}+Y_{C_0\min}}{2}-Y_{O_2}\right)\\ +\left(X_{C_h\max}-X_{C_0\min}\right)\left(\dfrac{X_{C_h\max}+X_{C_0\min}}{2}-X_{O_2}\right)\end{bmatrix}d\theta_1 \quad (15)$$

The instantaneous flowrate, $Q(t)$, can be expressed as follows:

$$Q(t)=\lim_{\Delta t\to 0}\frac{\Delta V}{\Delta\theta_1}\frac{\Delta\theta_1}{\Delta t}$$
$$=\omega_1 b\begin{bmatrix}\left(Y_{C_h\max}-Y_{C_0\min}\right)\left(\dfrac{Y_{C_h\max}+Y_{C_0\min}}{2}-Y_{O_1}\right)\\ +\left(X_{C_h\max}-X_{C_0\min}\right)\left(\dfrac{X_{C_h\max}+X_{C_0\min}}{2}-X_{O_1}\right)\end{bmatrix}$$
$$-\frac{m-1}{m}\omega_1 b\begin{bmatrix}\left(Y_{C_h\max}-Y_{C_0\min}\right)\left(\dfrac{Y_{C_h\max}+Y_{C_0\min}}{2}-Y_{O_2}\right)\\ +\left(X_{C_h\max}-X_{C_0\min}\right)\left(\dfrac{X_{C_h\max}+X_{C_0\min}}{2}-X_{O_2}\right)\end{bmatrix} \quad (16)$$

where ω_1 is the angular velocity of the inner rotor and t is the time.

The average flowrate, Q_{avg}, can be expressed as follows:

$$Q_{avg} = \frac{V_{2\pi}}{2\pi}\omega_1 \tag{17}$$

3. Contact points of the inner and outer rotors

The motion of the rotors comprises the rotation of the inner rotor, θ_1, and that of the outer rotor, θ_2, as shown in Fig. 1. The instantaneous displacement of the pitch point, $\vec{p}$, at the center of the inner rotor, O_1, coincides with the displacement at the center of the outer rotor, O_2.

$$r_1\theta_1 = r_2\theta_2 \tag{18}$$

Because the proportion of r_1 to r_2 is proportional to the number of lobes of the inner and outer rotors,

$$\theta_1 = \frac{m}{m-1}\theta_2 \tag{19}$$

The contact points at these respective lobes are the points at which the line connecting the center of the circular arc gear profile of the outer rotor to the pitch point meets the circular arc gear profile curve, as shown in Fig. 1. The center coordinate of the circular part of the outer rotor, $\overrightarrow{S_k}$, varies with the rotation angle, θ_2, and can be expressed as follows:

$$\begin{aligned}\overrightarrow{S_k} &= X_k\vec{i} + Y_k\vec{j} \\ &= r_t\cos\left(\frac{2k}{m}\pi+\theta_2\right)\vec{i} + r_t\sin\left(\frac{2k}{m}\pi+\theta_2\right)\vec{j}\end{aligned} \tag{20}$$

where $\vec{i}$ and $\vec{j}$ are the unit vectors in the horizontal axial and vertical axial directions, respectively. r_t is the distance from the axis, O_2 of the outer rotor to the center of the circular part.

The coordinates of the pitch points, which are fixed points, are

$$\vec{p} = me\vec{i} + 0\vec{j} \tag{21}$$

where e is the eccentricity between the centers of the inner and outer rotors. The $\overline{pS_k}$ linear equation connecting the pitch point to the center coordinate of the circular part of the outer rotor, $\overrightarrow{S_k}$ is as follows:

$$\begin{aligned}Y &= \frac{Y_k}{X_k - me}(X - me) \\ &= \frac{r_t\sin\left(\frac{2k}{m}\pi+\theta_2\right)}{r_t\cos\left(\frac{2k}{m}\pi+\theta_2\right) - me}(X - me)\end{aligned} \tag{22}$$

The circular equation of the outer rotor with S_k as the center is as follows:

$$(X - X_k)^2 + (Y - Y_k)^2 = r_c^2 \tag{23}$$

where r_c is the radius of the outer rotor's circular part.

The intersection points of equations (22) and (23) become the contact points, C_k.

4. Numeric examples

Based on equations (11) - (23), the instantaneous volume change rate, flowrate, torque, and rotation speed were calculated via a MATLAB program code. The gerotor considered in the numeric example was the case in which the inner and outer rotors rotated with respect to the fixed axes.

Table 1 lists the basic specifications of the gerotor pump/motor used for the numerical analysis, and Fig. 6 shows the profiles of the inner and outer rotors of the basic specifications. Additionally, Fig. 6 shows the states of the inner and outer rotors at the rotation angle of 0° in the inner rotor. Fig. 7 shows the flowchart of the MATLAB program.

Table 1 Specifications of gerotor pump/motor used in numerical analysis

Item	Data (mm)
Number of outer rotor lobes	4
Number of inner rotor lobes	3
Eccentricity (e)	2.5
Radius of circular part of outer rotor (r_c)	6.5
Distance of O2 - Sk (r_t)	16.5
Rotor thickness (b)	1.5

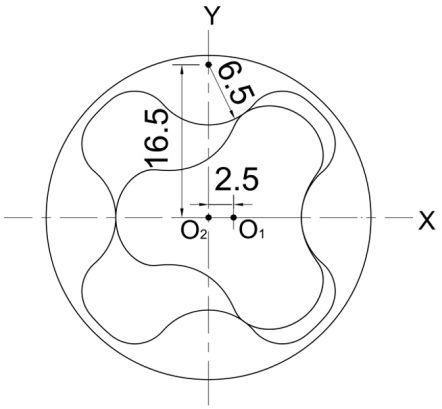

Fig. 6 Profiles of the inner and outer rotors used in the analysis

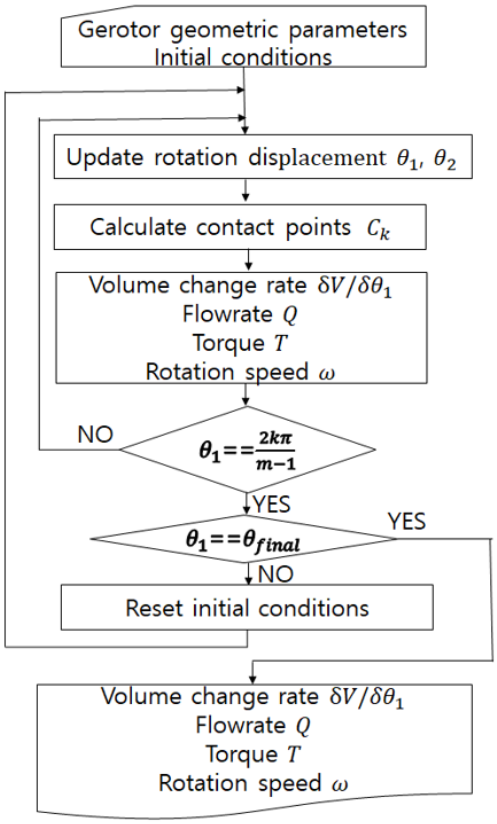

Fig. 7 Flowchart to calculate numeric values

Fig. 8 illustrates a graph of the volume change rate based on equation (13) in Section 2.3. The data values on the horizontal axis are the rotation angles of the inner rotor, θ_1, and at the point where θ_1 is ± 0.5818 rad, the volume change rate is identical to the average volume change rate of 69.74 mm^3/rad. The value multiplied by 2π is the volumetric displacement per revolution, which is calculated to be 438.19 mm^3/revolution.

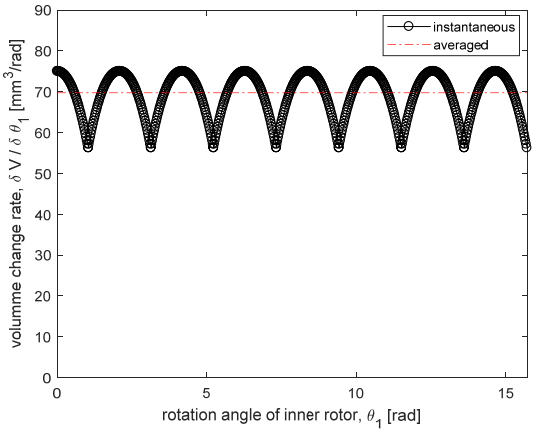

Fig. 8 Plot of volume change rate

The maximum value of the volume change rate is 75.0 mm^3/rad when the rotation angle of the inner rotor, θ_1, is zero. The minimum volume change rate is 56.25 mm^3/rad at θ_1 of 1.047 rad. The maximum fluctuation from the average value is $+7.54$ %, whereas the minimum fluctuation is -19.34 %.

The instantaneous flowrate discharged from a pump can be calculated from equation (16). Figs. 9 and 10 illustrate the flowrates for two cases: when the pump driving shaft speeds are 183.26 rad/s (or 1750 rpm) and 122.52 rad/s (or 1170 rpm). Figs. 9 and 10 show plots of the instantaneous pump flowrate with respect to the rotation angle of the inner rotor θ_1 and time, respectively. These figures are similar to Fig. 8. All the fluctuation ratios of the instantaneous pump flowrate are the same as that of the volume change ratio, which is shown in Fig. 8.

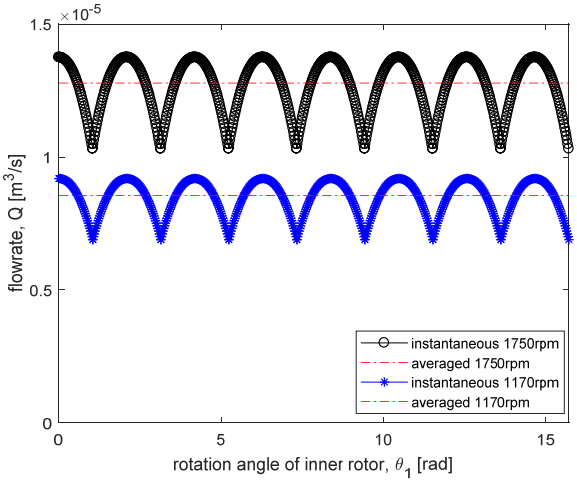

Fig. 9 Plots of pump flowrates with respect to rotation angle of inner rotor

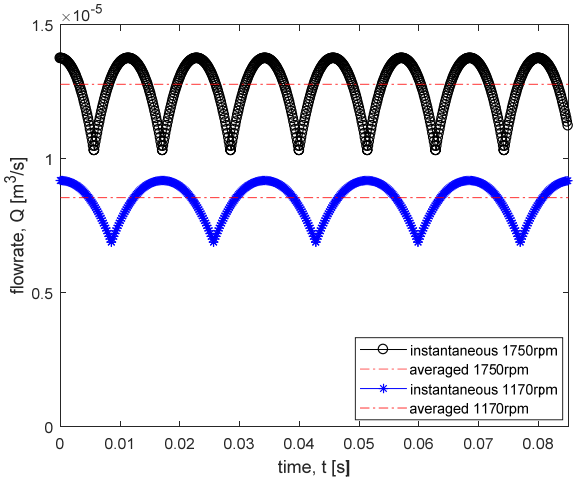

Fig. 10 Plots of pump flowrates with respect to time

Equation (16) may be used to calculate the instantaneous rotation speed of a gerotor-type motor. Hydraulic fluid was assumed to be incompressible and the pressure in a relief valve was set much higher than the normal range of working pressure of the gerotor motor, that is, the inertia load pressure was negligibly small. The flowrate supplied into the motor was assumed to be constant. Under these assumptions, the instantaneous speed of the motor can be expressed as follows:

$$\omega(t) = \frac{d\theta_1}{dt} = Q(t) / \frac{dV}{d\theta_1} \tag{24}$$

Figs. 11 and 12 show plots of the instantaneous motor rotation speed with respect to the rotation angle of the inner rotor, θ_1 and time, respectively. Figs. 11 and 12 illustrate the flowrates for two cases: when the motor flowrates are 3.33×10^{-4} m^3/s (or 20 lpm) and 1.67×10^{-4} m^3/s (or 10 lpm). The shape of the motor speed fluctuation resembles a upside down shape of Fig. (8) - (10). This is because the motor speed is inversely proportional to the volume change rate, $dV/d\theta_1$.

The output torque of a motor can be calculated from equation (11). Figs. 13 and 14 illustrate the load torques acting on a motor shaft for two cases: when the supply pressures to the motor are 100×10^5 N/m^2 (or 100 bar) and 70×10^5 N/m^2 (or 70 bar).

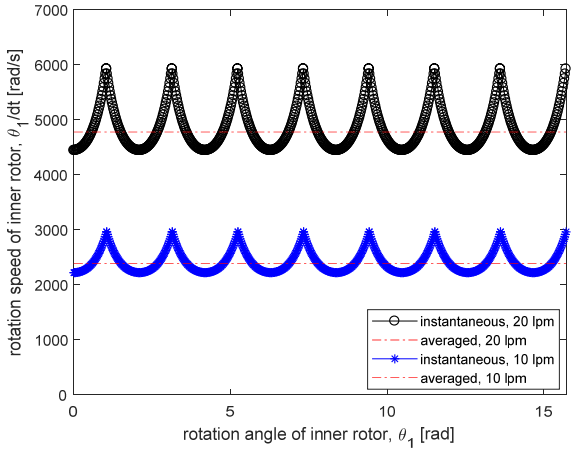

Fig. 11 Plots of motor rotation speed with respect to rotation angle of inner rotor

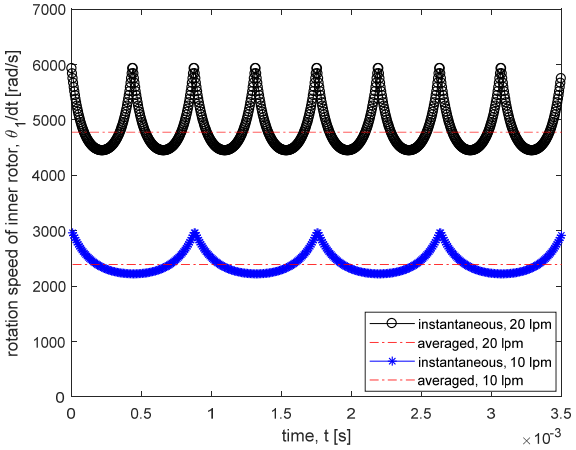

Fig. 12 Plots of motor rotation speed with respect to time

Figs. 13 and 14 show plots of instantaneous motor torques with respect to the rotation angle of the inner rotor, θ_1 and time, respectively. The main features of these figures are similar to those of Fig. 8 - 10.

If equation (11) is transformed to the following equation (25), the equation may be applicable to calculate the instantaneous outlet pressure of a gerotor-type pump when the input torque is assumed to be constant.

$$P(t) = T(t) / \frac{dV}{d\theta_1} \tag{25}$$

where the volume change rate $dV/d\theta_1$ is given as equation (13). Equation (25) is a static relation and the pump should rotate at a low speed such that equation (25) can be used reasonably.

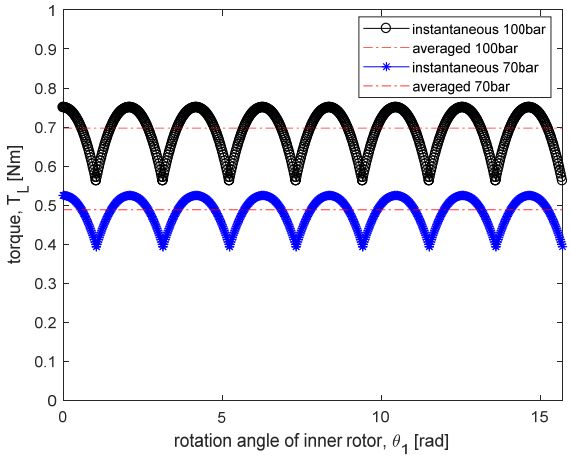

Fig. 13 Plots of motor output torque with respect to rotation angle of inner rotor

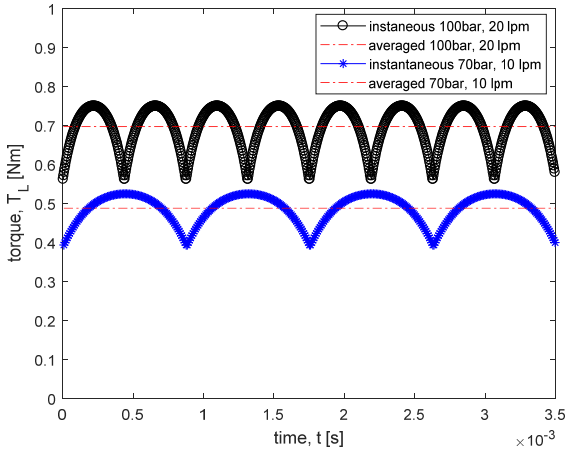

Fig. 14 Plots of motor output torque with respect to time

However, typical pumps are operated at high speeds and the outlet pressure should be set dynamically based on the flow continuity of the outlet volume, pumping flowrate fluctuation, fluid compressibility, etc. Therefore, equation (25) may be meaningless when real pumps are used.

5. Conclusion

This study proposed a method for calculating the instantaneous volume change rate, flowrate, rotation speed, and torque of pumps/motors based on two basic concepts: the torque equilibrium of rotors and the energy conservation between the hydraulic energy of pumps/motors and mechanical energy of driving shafts. The contact points between the inner and outer rotors should be calculated in the calculation process of the volume change rate, rotation speed, and torque of the pump/motor. A series of responses of the instantaneous volume change rate, rotation speed, and torque of pumps/motors was illustrated for specific geometric parameters of a gerotor shape. However, those calculated responses may show some errors from real responses because the inertia of the pump/motors and compliance effect of oil are not considered in those torque equilibrium and energy conservation equations.

Acknowledgement

This research was supported by Kumoh National Institute of Technology (grant number 2019-104-048).

Conflicts of Interest

The authors declare that there is no conflict of interest.

References

1) J. R. Colbourne, "The Geometry of Trochoid Envelopes and their Application in Rotary Pumps", Mechanism and Machine Theory, Vol.9, pp.421-435, 1974.
2) C. B. Tsay and C. Y. Yu, "Mathematical Model for the Profile of Gerotor Pumps", Journal of the Chinese Society of Mechanical Engineers, Vol.10, No.1, pp.41-47, 1989.
3) D. W. Dudley, Handbook of Practical Gear Design, McGraw-Hill, New York, pp.1-33, 1984.
4) H.-S. Jung, Y. M. Lim and Y.-B. Ham, "New Tooth Type Design and Characteristic Analysis for High Density Gerotor Pump", Journal of Drive and Control, Vol.16 No.4, pp.80-86, 2019.
5) J. R. Colbourne, "Gear Shape and Theoretical Flow Rate in Internal Gear Pumps", Transactions of the Canadian Society for Mechanical Engineering, Vol.3, No.4, pp.215-223, 1975.
6) S.-C. Lee, "Profile Design of the Inner Rotor of a Gerotor by the Composite Curve of Circular Arcs",

Journal of the Korean Society of Tribologists and Lubrication Engineers, Vol.22, No.2, pp.79-86, 2006.

7) J. C. Kim, J. H. Shin, and S. M. Kwon, "A Study on Gear Tooth Profile of a Positive Displacement Rotor Pump", Proceedings of the Korean Society of Machine Tool Engineers, Fall Conference, pp.106-111, 2006.
8) S. D. Kim et al., "An Analysis on Volumetric Displacement of Gerotor Pump/Motor Using Vane Length", Transactions of the Korea Fluid Power Systems Society, Vol.8, No.2, pp.8-16, 2011.
9) N. D. Manring and S. B. Kasaragadda, "The Theoretical Flow Ripple of an External Gear Pump", Journal of Dynamic Systems, Measurement, and Control, Vol.125, No.3, pp.396-404, 2003.
10) D. C. H. Yang, J. Yan, S.-H. Tong, "Flowrate Formulation of Deviation Function Based Gerotor Pumps", Journal of Mechanical Design, Vol.132, 064503, 2010.
11) D. C. H. Yang, Jia Yan and S.-H. Tong, "Flowrate Formulation and Displacement Analyses for Deviation Function-based Gerotor Pumps", Proceedings of the Institution of Mechanical Engineers, Part C: Journal of Mechanical Engineering Science, Vol.225, pp.480-487, 2010.
12) K. J. Huang and W. C. Lian, "Kinematic Flowrate Characteristics of External Spur Gear Pumps using an Exact closed Solution", Mechanism and Machine Theory, Vol.44, pp.1121-1131, 2009.
13) S. W. Choi, C. D. Lee and S. Y. Yang, "A Study on Simulation of Piston Number for Development of Axial Piston Pump for Wheeled Armored Vehicle", Journal of Drive and Control, Vol.16, No.1, pp.14-21, 2019.